Two-Dimensional Equatorial Electrojet Current System Deduced from the Brazilian Network : 1. Based on the H component

Colqui, R
Faculty of Sciences, Kyushu University

Yumoto, Kiyohumi
Faculty of Sciences, Kyushu University

Tachihara, Hiroshi
Faculty of Sciences, Kyushu University

Kitamura, T-I
Faculty of Sciences, Kyushu University

他

https://doi.org/10.5109/1546076

出版情報：九州大学大学院理学研究院紀要 : Series D, Earth and planetary sciences. 30 (1), pp.1-14, 1998-01-30. Faculty of Science, Kyushu University
バージョン：
権利関係：

Mem. Fac. Sci., Kyushu Univ., Ser. D, Earth Planet. Sci., Vol. XXX, No. 1,
pp. 1-14, text-figs. 1-10, tables 1-2, January 30, 1998

Two-Dimensional Equatorial Electrojet Current System Deduced from the Brazilian Network

I. Based on the H component

R. COLQUI, K. YUMOTO, H. TACHIHARA, T-I KITAMURA N. B. TRIVEDI*
and José Marques DA COSTA*

Abstract

In order to investigate the dynamical behavior of the EEJ current system from its effects on ground based magnetic records, data from two low-latitude chains on the Brazilian sector was used. A quasi-simulated calculation method was developed to determine the current intensity distribution inside the EEJ. The resulting current distribution obtained using only the H component of the records reproduces quite well the observed temporal variations of the magnetic field. The analysis of the calculated current system shows that the EEJ in many cases has a double structure during the morning evolving into the classical "single structure" around noon when the effect of the EEJ is maximum.

1. Introduction

The establishment of a geomagnetic observatory at Huancayo (Peru) near the equator revealed an abnormally large amplitude of Sq variation in the horizontal component H (northward). The study of this anomaly revealed a strong electric current flowing eastward approximately along the magnetic equator at ionospheric E-layer height. This eastward current has been called Equatorial ElectroJet (EEJ) by CHAPMAN (1951).

Since its discovery, the EEJ has proven to be a fascinating geophysical phenomenon and many people have investigated different aspects of the EEJ in the last decades, nevertheless, many facets of it still continue to elude our understanding. Nowadays we can think the EEJ current as the consequence of electromotive forces produced by disturbances in the lower atmosphere on a local and global scale, as well as disturbances originated in the solar wind -magnetosphere-ionosphere interactions.

One of the main goals of the present study was to investigate the dynamical behavior of the EEJ current during quiet days.

2. The Equatorial Electrojet (EEJ)

2.1 Nature of the EEJ

The direction of the geomagnetic field changes from horizontal at the magnetic dip equator to vertical at the magnetic poles. A horizontal east-west electric field can then drive

Manuscript received September 10, 1997; accepted October 31, 1997.

* Instituto Nacional de Pesquisas Espaciais, São José dos Campos São Paulo, Brazil

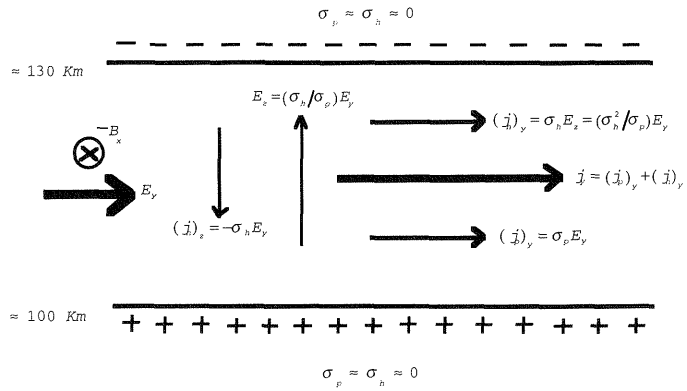

Fig. 1. The Equatorial Electrojet in a slab geometry. The conductivity outside the slab is assumed to be zero.

horizontal Pedersen and Hall currents which are related to the electric field as

$$j=\sigma \cdot E \quad \text{with} \quad \sigma=\begin{pmatrix} \sigma_p & \sigma_h \\ -\sigma_h & \sigma_p \end{pmatrix}$$

The conductivity parallel to E but orthogonal to B_0, which is called the Pedersen conductivity σ_p is mainly due to the ions. The conductivity orthogonal to both E and B_0, mainly due to electrons, is called the Hall conductivity σ_h.

At the dip equator the Pedersen current flows in the y (eastward) direction $[(j_p)_y=\sigma_p E_y]$ and the Hall current flows in the vertical (z) direction $[(j_h)_z=-\sigma_h E_y]$.

Since the vertical current can not flow out of the dynamo region, a polarization charge causes a vertical electric polarization field $[E_z=(\sigma_h/\sigma_p)E_y]$ to compensate the Hall field, so that finally no vertical current flows $[j_z=0]$.

This 'secondary' vertical field, however, drives a horizontal Hall current $[(j_h)_y=\sigma_h E_z=(\sigma_h^2/\sigma_p)E_y]$ in the y direction which adds to the primary Pedersen current. This enhancement of the current about the magnetic dip equator is known as the EEJ and can be described by the Cowling conductivity σ_c;

$$j_y=(j_p)_y+(j_h)_y,$$
$$j_y=\sigma_c \cdot E_y,$$
$$\sigma_c=\sigma_p+\frac{\sigma_h^2}{\sigma_p}$$

For many applications, the dynamo region can be approximated by a thin homogeneous layer of thickness $\Delta h \approx 50$km.

2.2 Empirical models

The numerical and physical models of the Equatorial Electrojet have not yet developed to the point of being used in the analysis of the observed data, consequently, all electrojet observed data in most of the cases have been analyzed with empirical models.

Some investigators have used the line current model (FORBUSH and CASAVERDE, 1961; HESSE, 1982), some have used the model of a current band or ribbon of constant intensity

(ONWUMECHILI, 1959; OSBORNE, 1962; CAIN and SWEENEY, 1972) and others have used a divergent or open-ended model (FAMBITAKOYE and MAYAUD, 1976) like the parabolic or the fourth degree model in which the current intensity quickly decreases in magnitude, with distance from the magnetic dip equator but this is arbitrarily truncated at some distance for the purpose of using the more modest intensites to fit the electrojet.

Those models succeed in providing a rough description of the EEJ but present some important limitations, for example, the observational data along latitudinal profiles across the EEJ showed that none of these models fitted the observations well.

2.3 The present approach

It is generally accepted that at the magnetic dip equator the earth's magnetic field is horizontal and generally northward. On the other hand the stratification of the ionosphere restricts the currents to flow primarily in horizontal layers. Therefore it was assumed that the principal EEJ current flows horizontally and approximately perpendicular to the magnetic field.

2.3.1 The coordinate system

Assumed on the basis of the geometry described in 2.1, was a rectangular coordinate system (x, y, z) such that the $x-y$ plane is parallel to the ground with the positive z axis pointing downward, the y axis is along the dip equator with its positive derection being eastward and the x axis pointing to the north.

Even there is more complicated coordinate systems which use invariant latitude and longitude (or magnetic local time), in this study, based on the modeled geomagnetic field configuration, it is considered that at the geomagnetic dip equator the differences between such other coordinate systems and the assumed here, are irrelevant.

2.3.2 The region of analysis

In order to chose the placement of the region to be analyzed we have taken into account

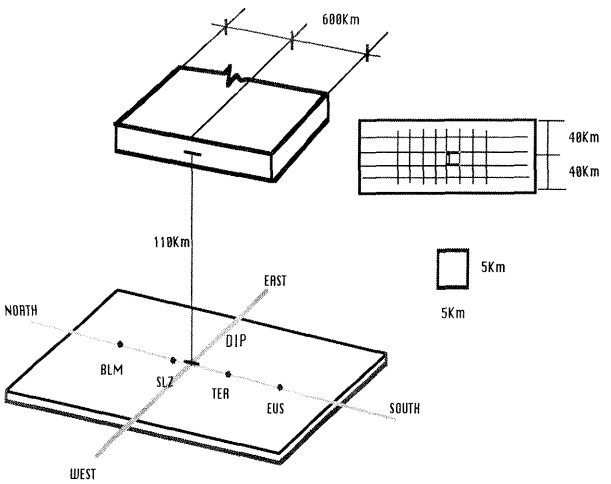

Fig. 2. Schematic illustration of the region of analysis, its cross section, the cells inside the region and the dimensions of one cell.

the following results from previous studies. First, radar observations in Peru suggest that the maximum polarization field at the equator occurs at about 104 km altitude (FEJER *et. al.*, 1975). Second, rocket observations (e. g., DAVIS *et al.*, 1967 ; MAYNARD, 1967 ; SHUMAN, 1970) indicate that the peak current density at the equator occurs at about 107 km. Third, electrojet measurements from satellite (e. g., OSBORNE, 1973) indicate that the signature 'half-width' of the electrojet over Peru is 260 ± 25 km which is similar to the suggested by FORBUSH and CASAVERDE (1961).

Then, on the basis of the results outlined above, we have chosen as the region of analysis (Fig. 2), a thick ribbon shaped space, wide and thick enough to contain the EEJ.

The center of the region was located at 110 km of altitude just over the ground with its axis parallel to the dip equator. The width was chosen as 600 km (North-South) and its thickness 80 km (up-down).

Under the consideration that the current flows in isolated tubes, the region of analysis was divided in small tubes with square cross section of 5 km side, therefore the EEJ current system can be easily represented by a two dimension matrix whose elements have to be calculated.

2.3.3 Approaching a model

The model used in the calculations is mainly based in the magnetic effect produced by an infinite line of current with intensity i, flowing horizontally and approximately along the dip equator somewhere inside the region of analysis. This field is used to calculate by superposition the magnetic effect of a ribbon of lines of current with some distribution of intensities. Finally, because of its linearity, the magnetic effect of many ribbons are superposed to obtain the total X component of the magnetic field produced by an array of currents confined in a rectangular region as described before.

The analytical expressions used to calculate the magnetic field of a line of current with the geometry descirbed above are :

$$dB_x = KI \frac{110m\,dt - mz_{lc}\,dt}{(m^2t^2+(x_{op}-x_{lc}-t)^2+(110-z_{lc})^2)^{\frac{3}{2}}}$$

which is integrated to obtain

$$B_x = KI \frac{2|m|(110-z_{lc})\sqrt{1+m^2}}{m^2[(x_{lc}-x_{op})^2+(110-z_{lc})^2](110-z_{lc})^2},$$

If the inclination of the line of current with respect to the dip is zero the expression for the X component of the geomagnetic field becomes

$$m\to\infty \Rightarrow (B_{xp},\ B_{yp},\ B_{zp}),$$

$$B_{xp} = KI \frac{2(110-z_{lc})}{(x_{lc}-x_{op})^2+(110-z_{lc})^2}$$

This expression is mainly used in the calculations.

3. Method of analysis

3.1 Calculation Method

The determination of the 'best' solutions to certain mathematically defined problems,

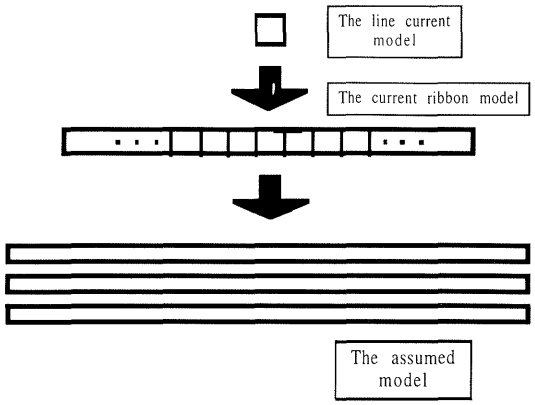

Fig. 3. Schematic illustration of the calculation method. The arrows indicate how the calculation method evolves, starting with the well known 'line current model' until finally get an array of many "current ribbons" models.

which are often models of physical reality, falls into the domains of the science of optimization. It involves the study of optimality criteria for problems and the determination of algorithmic methods of solution. There are therefore a wide range of possibilities some of these having a considerable effect on the performance of the method.

In this sense, determining the 'best' system of currents capable of simulating as close as possible the observed X component of the geomagnetic field at all the observation points for every set of sampled data, is the statement of the problem.

As for the optimization, the criteria on which the method is based is the minimization of the difference between the X component produced by the system of currents flowing inside the region of analysis on every observation point and the observed values of the same component on those points. This can be expressed by

$$err_{tot}=\sqrt{err^2_{op1}+err^2_{op2}+\cdots+err^2_{opn}}$$

With respect to the direction on which the current flows, it must be mentioned that there is no imposed restriction which means that the intensity of current can be positive (eastward), negative (westward), or zero according the necessities of the data to be explained.

The determination of the intensities of every line of current is carried out in an order that resembles the evolution of the electrojet models.

The process starts with a single line of current with which is intended to explain the data, naturally as it is not enough another line of current is added to the system, the process continues until all the 'tubes' of the sheet are completed. The calculation then resumes with another layer and the process is repeated until cover all the layers inside the region of analysis as can be seen in Fig. 3.

3.2 The algorithm

At this point it must be mentioned that usually one approaches an optimization problem

presupposing that the minimizer value exists, is unique, and is located by the used algorithm. Whilst this is often the case, it is important to realize that there are cases in which this ideal situation may fail. Therefore the difficulties in guaranteeing to find the 'best' solution are considerable.

3.2.1 The 'direct search' algorithm

Even though the amount of effort required to find the solution is big, the algorithm chosen to fit the intensities of current to the observed data is the called 'direct search' algorithm in which the searching of the solution is made by a large number of trials.

The 'direct search' is an iterative method which generates a sequence of estimates of the solution. The sequence terminates when an iterate is located which satisfies some imposed conditions.

In the present case it is not necessary to supply an initial estimate of the solution to start the calculations since the initial intensity is assumed to be zero. As it is shown in Fig. 3, the basic structure of the kth iteration is

(a) determine the direction of search $i_{mn}^{(k)}$

(b) find $i_{mn}^{(k)}$ to minimize err_{tot}

(c) set $i_{mn}=i_{mn}^{(k)}$

The determination of the direction of search for the kth iteration is based on the comparison between the errorINC or errorDEC and the errorMIN. This means that if the error produced by an increment of the intensity is less than the produced by a decrement then

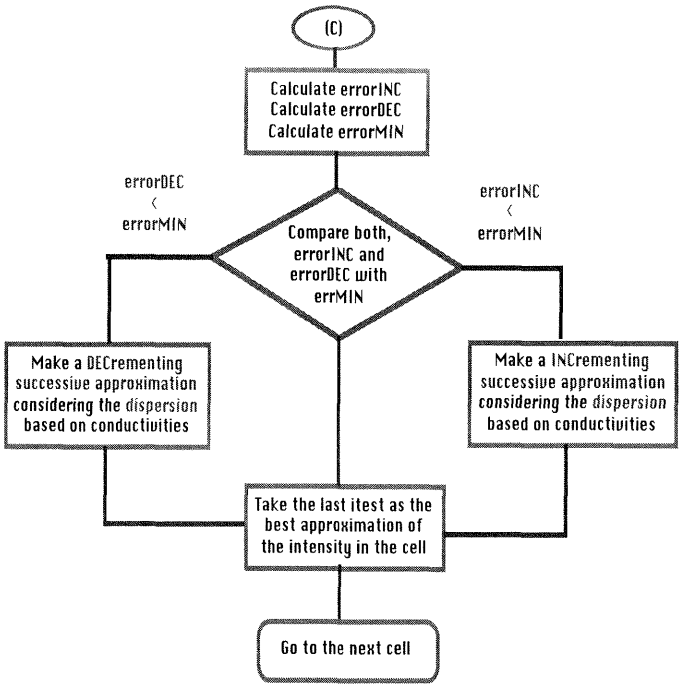

Fig. 4. Flowchart of the algorithm to fit the intensity of current of one line to the observed data. The direction of search is determined by comparing the errorINC or errorDEC with the errorMIN.

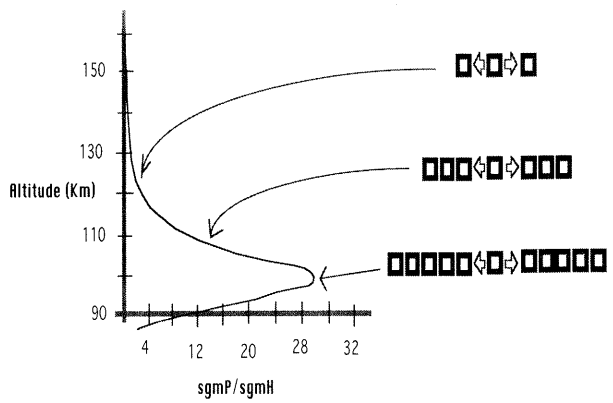

Fig. 5. The dispersion of the tested intensity of current according the vertical profile of conductivities.

the search must be done using successive INCrements of $i_{mn}^{(k)}$, otherwise the approximation must be done using successive DECrements of $i_{mn}^{(k)}$.

To find the $i_{mn}^{(k)}$ which minimizes the err_{tot}, a method that resembles the well known 'successive approximation' algorithm of the A/D converters was used because it is faster and easy to implement.

The approximation process is not continuous, the trials are done using at first 'big' steps for the successive INCrements or DECrements and then the steps are reduced according the necessities of the values to be fitted. If the resulting intensity is greater than the maximum allowed value, the algorithm performs a 'dispersion' of the tested intensity and the trial continues with another step smaller than the previous one. This process continues until all the step values have been used.

3.2.2 The dispersion based in conductivities

This is a procedure executed in case the increment or decrement of intensity $i_{mn}^{(k)}$ goes beyond the allowed limits. In this case, as the Fig. 5 shows, the test intensity is 'dispersed' (divided) into n horizontally adjacent tubes. The number n is determined according the vertical profile of the relation $[\sigma_P/\sigma_h]$.

4. The Brazilian Network

The Brazilian Network is part of the equatorial magnetic network stations, which are conducted by the Department of Earth and Planetary Sciences of Kyushu University, under the equatorial magnetic network project (STEP) in cooperation with

Instituto de Nacional Pesquisas Espaciais (Brasil),
University of Victoria (Canada),
University of British Columbia & (Canada),
University of California San Diego (U. S. A),
Instituto Geofisico del Peru (Peru).

The magnetic observations were also supported by the following institutions:

EMBRAPA (Teresina, Brasil),

Universidade Federal de Santa Maria (Santa Maria, Brasil)
CNPq (Belem, brasil)

4.1 The Stations

The Brazilian Network consists of two chains of magnetometers located in the east and west side of the Brazilian territory.

4.2 Instrumentation

The magnetometers used in all the stations are based on the fluxgate technology and are capable of producing high quality digital output which can be stored in audio tapes or flash memory cards.

Table 1

Sta. Name	Code	Geographic		Geomagnetic		
		Lat.	Long.	Lat.	Long.	Inc
Belem	BLM	-1.17	-48.48	9.01	22.72	8.152
SaoLuiz	SLZ	-2.60	-44.20	1.24	26.91	0.799
Teresina	TER	-5.02	-42.5	4.68	28.39	-5.56
Eusebio	EUS	-3.52	-38.26	5.76	32.76	-7.964

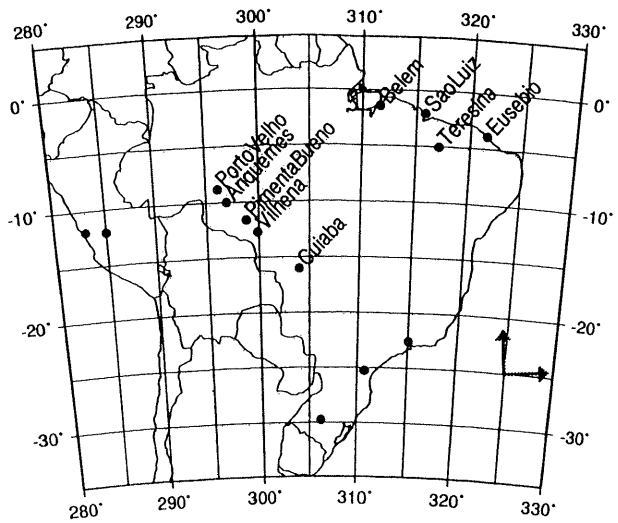

Fig. 6. Stations used in the study: BLM, SLZ, TER, EUS. The grid corresponds to a geographic coordinate system (from GMT).

Table 2

sensor	Three ring cores
components X,Y,Z,	three components
noise level	0.015 nT/Hz$^{(1/2)}$
sampling	3 sec
time keeping	less than 100 ms, (auto correction)
recording system	1. memory card
	2. walkman cassette recorder
recording media	1. 4 MB (46 days)/20M (230 days)
	memory card
	2 music tape (14 days/side)
power consumption	3 watts max.
power supply	AC100-240/solar battery with
	floating system

The instruments have been designed and assembled completely in the Department of Physics, Kyushu University to satisfy the requirements of portability, easy of installation, and low power consumption. It can operate independently for about six months.

The main features of the magnetometers are given in table 2.

4.3 Data handling

To minimize the effects of purely seasonal origin the data have been confined to only one season. On the other hand, due to availability of the simultaneous observations, the month chosen for the analysis was April, 1993. The data were taken from four stations located across the dip equator in a nearly symmetric arrangement. Two of them are on the magnetic North (BLM, SLZ) and the other two on the magnetic South (TER, EUS).

To be able to study the effect of the hour-to-hour variation of the electrojet, it was necessary to determine the EEJ strength. Therefore, for each day at each station, a zero level was determined by interpolating linearly between the levels of the records of each of the nights neighboring the day considered.

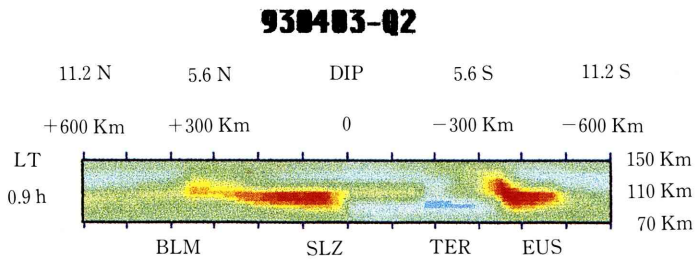

Fig. 7. Distribution of the equatorial electrojet current density obtained by fitting the intensities to the observed X component of the geomagnetic field.

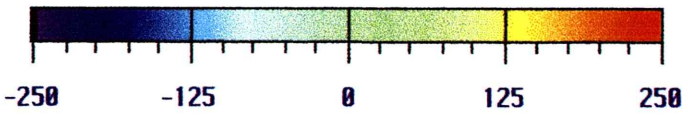

Fig. 8. Coded color scale for the intensities of current flowing inside one tube in Amperes/25 km^2.

5. Results

5.1 Presentation format

The advantages of a graphic presentation of the current intensities of the equatorial electrojet are so obvious that it has often been attempted even when the available data are not ideal. Among the earliest attempts are those of ONWUMECHILI (1965) and SUGIURA and CAIN (1966). For example SUGIURA and POROS (1969) presented contours of equal density with some indications of westward currents on the flanks of the dip equator.

In the present case, results of the calculations are showed not in a contour form but in a color coded intensity distribution whose scale is explained in the next section as can be seen in Fig. 7.

To make easy the interpretation of the figure there are adjoined some annotations whose meaning will be explained.

The title format is "YYMMDD-Activity", YY for the year, MM for the month, DD for the day and 'Activity' for the level of magnetic activity (Q=quiet, D=disturbed). The local time is placed at left in 24-hours format, the horizontal axis represents distance from the dip in kilometers, positive values mean northward and the negative values southward, there is an additional horizontal scale which means geomagnetic latitude degree.

The numbers placed at right represent the heights of the bottom, top, and center of the analyzed region respect to the ground, thus, the bottom layer is at 70 km, the top layer is at 150 km.

5.2 Representation of the intensities

The current intensity flowing inside one 'tube' is represented by a coded color scale as showed in Fig. 8.

Notice that the scale in in Amp/25 km^2, so if the scale indicates a intensity of 250 the current density at that point will be 10 Amp/km^2. Positive values indicates currents flowing eastward and the negatives ones westward currents.

6. Discussion

6.1 Quietest days

It is important to be sure that the observed magnetic field is caused only by the EEJ and not by another sources, and therefore it is important to know when the contribution of other sources is minimum or null.

On quiet days, the other sources of magnetic disturbance are small or are weak enough to be considered small, so we can assume that the observed values of the field are due mainly to the EEJ.

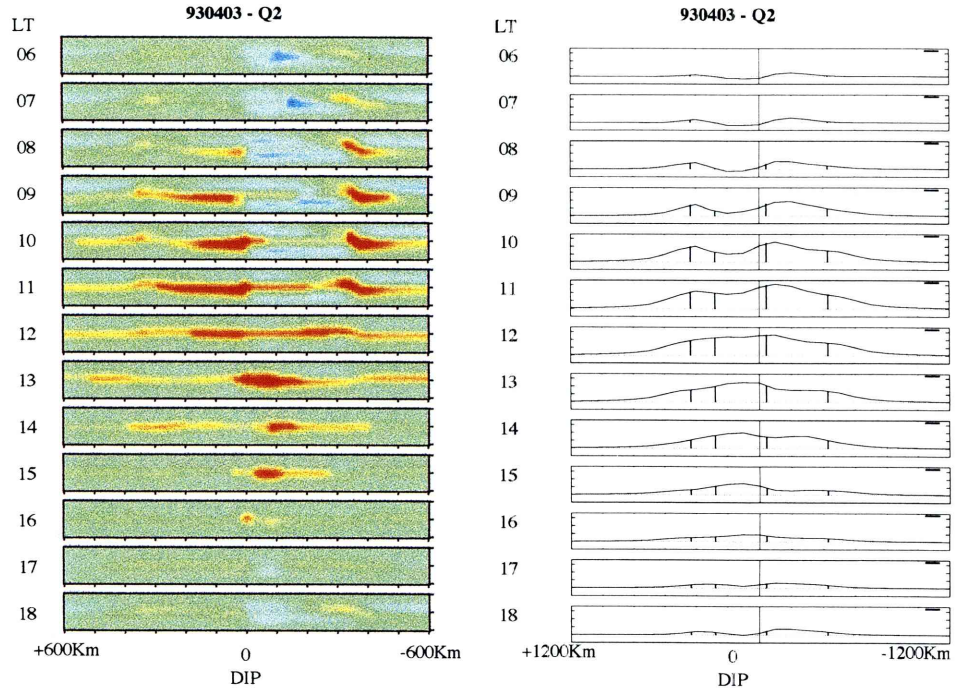

Fig. 9. Current intensity pattern (left) and calculated (continuous line) and observed (bars) latitudinal profiles for 93-04-03.

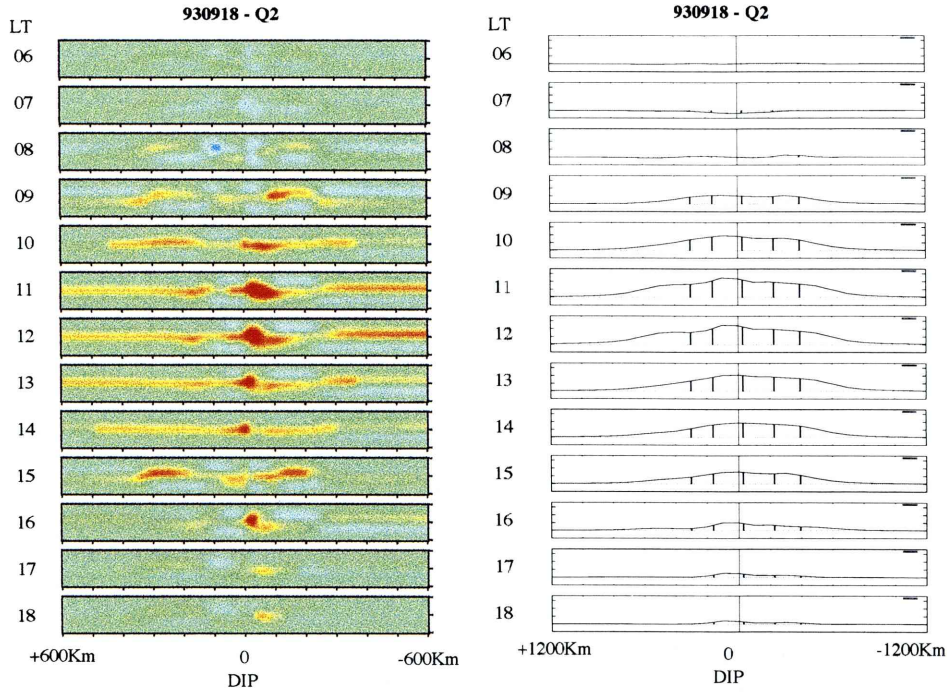

Fig. 10. Current intensity pattern (left) and calculated (continuous line) and observed (bars) latitudinal profiles for 93-09-18.

Although the calculation was made for the other quiet days the results shown in the present case correspond to the second quietest days of April and September 1993 (Figures 9 and 10). The first one is designated 930403-Q2 (Figure 9) and the last one is designated 930918 -Q2 (Fig. 10). Together with the current density, an hourly latitudinal profile produced by the calculated system of currents and the observed X component of the geomagnetic field were included.

Notice the formation of two centers of high current density on the sides of the dip at 0800 LT in the chart for 930403-Q2. As time passes, the two structures become more intense and finally merge into one structure around 1200 LT.

In the chart for 930918-Q2, the formation of two centers is not as clear as in the previous case, but we can observe a typical EEJ development with a multiple structure starting at around 0900 LT and besoming strongest around 1200 LT.

Since the pattern observed for 930403-Q2 is not an isolated case but can be observed on many other days as well, we can think of the formation of two strong centers, one on each side of the dip in the morning, as a more or less regular feature in the development of the EEJ.

On the other hand, though there is no presupposition of the presence or absence of negative (westward) current, its presence is almost permanent because the fitting makes it positive or negative according the necessities of the data to explain. However most of the time the intensity of the westward current is much lower than the current flowing eastwards.

6.2 Consideration

An attempt to devise the model that agrees best with observations by empirically adjusting the distribution of current intensities yields a model in satisfactory agreement with the main features of the EEJ. It is necessary, however, to be cautions, because such an adjustment many have no particular physical significance. Further observational and theoretical research should help resolve this problem.

7. Conclusions

The results of the calculations presented in this work indicate that in many cases the EEJ presents a double structure during the first three or four hours of its development. This double concentration of high current intensity merge into one around noon showing the typical signature of the EEJ in the ground-based magnetograms.

During quiet days, the almost permanent presence of westward currents with very low intensity around the eastward main stream can be observed from the charts.

Another facts found in this study can be summarized in the following :

-It was presented a method for quantitatively estimating the distribution of current intensities that simulates the observed X component of the geomagnetic field on the observation points from ground based magnetograms.

-Even a new technique has been adopted to calculate the distribution of current intensities it is evident, from the plots of latitudinal profile and observed values, that the algorithm provides a good approximation at least on the points of observation.

-Even it is not easy to define the width of the EEJ, because it changes considerably with local time, it has minimal values (~250 km) around local noon as can be seen in the charts.

-In almost all days the EEJ evolves since a very narrow and weak system of currents in

the morning which becomes strong and wide as the time elapses. Normally the strongest and widest state is reached at around noon. Finally, in the afternoon the system of currents become weak and narrow until disappear.

-The system of currents obtained are non symmetric with respect to the dip equator as showed in the charts, on the other hand, the system of currents flow not precisely above the dip equator.

Acknowledgements

We are pleased to express our gratitude to F. X. Ogura and M. Okada of I. N. P. E for supplying the data utilized in the present study. R. Colqui at Kyushu University was supported by the Ministry of Education, Science, Sports and Culture of Japan.

References

FAMBITAKOYE O. and MAYAUD P. N. (1976a): Equatorial electrojet and regular daily variations S_R -I. A determination of the equatorial electrojet parameters. *Jour. Atmos. Terr. Phys.*, **38**, 1-17.

FAMBITAKOYE O. MAYAUD P. N. (1976b): Equatorial electrojet and regular daily variations S_R-II. The centre of the equatorial electrojet. *Jour. Atmos. Terr. Phys.*, **38**, 19-26.

FAMBITAKOYE O. and MAYAUD P. N. and RICHMOND A. D. (1976): Equatorial electrojet and regular daily variations S_R-III. Comparison of observations with a physical model. *Jour. Atmos. Terr. Phys.*, **38**, 113-121.

FAMBITAKOYE O. and MAYAUD P. N. (1976c): Equatorial electrojet and regular daily variations S_R -IV. Special features in particular days. *Jour. Atmos. Terr. Phys.*, **38**, 123-134.

FORBUSH S. and CASAVERDE M. (1961): Equatorial electrojet in Peru, Carnegie Institution of Washington, Publication No. 620, 135pp.

HESSE D. (1982): An investigation of the equatorial electrojet by means of ground-based magnetic instruments in Brazil. *Ann. Geophys.*, **38**, (3), 315-320.

KITAMURA T. I (1994): Daily Magnetograms (STEP), The equatorial magnetic network, April-June, 1992, AMERICAN SECTOR, Department of Physics, Kyushu University.

MAYAUD P. N. (1977): The equatorial counter-electrojet -a review of its geomagnetic aspects. *Jour. Atmos. Terr. Phys.*, **39**, 1055-1070.

ONWUMECHILI C. A. and AGU C. E. (1981): The relationship between the current and the width of the equatorial electrojet. *Jour. Atmos. Terr. Phys.*, **43** (5/6), 573-578.

OSBORNE D. G. (1962): Position and movement of the equatorial electrojet over Ghana. *Jour. Atmos. Terr. Phys.*, **24**, 491-502.

OSBORNE D. G. (1964): Daily and seasonal changes of the equatorial electrojet in Peru. *Jour. Atmos. Terr. Phys.*, **35**, 1097-1105.

OSBORNE D. G. (1973): Electrojet measurements from satellite and ground. *Jour. Atmos. Terr. Phys.*, **24**, 1273-1279.

RICHMOND A. D. (1973a): Equatorial electrojet -I. Development of a model including winds and instabilities. *Jour. Atmos. Terr. Phys.*, **35**, 1083-1103.

RICHMOND A. D. (1973b): Equatorial electrojet -II. Use of the model to study the equatorial ionosphere. *Jour. Atmos. Terr. Phys.*, **35**, 1105-1118.

REDDY C. A. (1981): The equatorial electrojet: a review of the ionospheric and geomagnetic aspects. *Jour. Atmos. Terr. Phys.*, **43**(5/6), 557-571.

SUGIURA M. and CAIN J. C. (1966): A Model Equatorial Electrojet. *Jour. Geophys. Res.*, **71**, (7), April 1, 1966.

VOLLAND Hans (1984): Electric Conductivity of Upper Atmosphere. In *Atmosphere Electrodynamics*. Springer-Verlag, Tokyo 1984.